Electronics and Communications in Japan, Part 2, Vol. 83, No. 4, 2000
Translated from Denshi Joho Tsushin Gakkai Ronbunshi, Vol. J82-C-I, No. 6, June 1999, pp. 310–317

Analysis of Electromagnetic Propulsion on a Two-Electric-Dipole System

Noriaki Obara

Communication Research Laboratory, Ministry of Posts and Telecommunications, Kashima, Japan 314-0012

Mamoru Baba

Faculty of Engineering, Iwate University, Morioka, Japan 020-8551

SUMMARY

This paper considers the electromagnetic propulsion of a body radiating directed electromagnetic waves. As the source of electromagnetic waves, a system consisting of two electric dipoles is chosen. The electromagnetic propulsion this system receives from the surrounding space is theoretically analyzed and discussed. This propulsion is related to the near field formed by the dipoles and exhibits the maximum propulsion at a characteristic dipole spacing. © 2000 Scripta Technica, Electron Comm Jpn Pt 2, 83(4): 31–39, 2000

Key words: Counteraction of radiation; photonic force; dipole; propulsion; near field.

1. Introduction

A force is exerted on an object emitting and absorbing electromagnetic waves. This force is called the "radiation reaction," "radiation pressure," or "photonic force" and has been known for a long time. In recent years, applications of the momentum of electromagnetic waves have been studied extensively due to advances in laser technology [1–10].

The authors have been interested in the propulsion of an object emitting directed electromagnetic waves by radiation reaction. An estimate of such an electromagnetic propulsion can be derived from balance computation of the macroscopic momentum between the electromagnetic wave and the object. Hence, the amount of the force applied to the object including the electromagnetic source can be derived from the momentum of the radiated electromagnetic wave. For instance, the reaction imparted to the laser source received by the emission of light can be estimated from the energy of the emitted light. It is not necessary to know the total contribution of each light-emitting atom in the source or the type of electromagnetic interaction. It is sufficient to consider the eventual momentum balance in a macroscopic sense between the source and the emitted light.

When one step further is taken from the computation of the macroscopic propulsion and it is instead considered as the sum of microscopic electromagnetic phenomena in the object (electromagnetic source), the question arises as to how these individual electromagnetic phenomena and the origin of the propulsion are exhibited. To the best of the authors' knowledge, there is no analytical study of the origin of such propulsion. In this paper, this electromagnetic propulsion is analytically derived in terms of a fundamental model and its implications are studied.

Although there are various sources of electromagnetic waves, one of the fundamental sources is a dipole. In a system with several electric dipoles or magnetic dipoles,

a directed electromagnetic wave is radiated due to the orientation and phase of each dipole. Then, propulsion is exerted on the system as the reaction to radiation. Such electromagnetic propulsion is derived from the momentum of the radiated electromagnetic field that is predominant at a distance sufficiently far among the electromagnetic field components generated in the surrounding space by the set of dipoles. On the other hand, the near fields, such as the static electric field and the inductive electromagnetic field, which constitute the remaining electromagnetic field components, have not been studied. In the present paper, as the most fundamental models for the analysis of electromagnetic propulsion, two types of systems consisting of two electric dipoles are considered. The results are studied with emphasis on the near field.

2. Analysis Models

2.1. Two fundamental analysis models

Let us consider dipole pairs consisting of two electric dipoles P_1 and P_2 separated by a distance d in a vacuum as shown in Figs. 1(a) and 1(b). In each system, the two dipoles have orientations parallel to the z axis. As shown in the following equations, the magnitudes $P_1(t)$ and $P_2(t)$ undulate with amplitudes of p_1 and p_2 at an angular frequency of ω and have phase difference of α $(0 \le \alpha < 2\pi)$:

$$P_1(t) = P_1 e^{j\omega t}$$
$$P_2(t) = P_2 e^{j(\omega t + \alpha)} \quad (1)$$

It is assumed that the spreading of the electric charge in each dipole is sufficiently smaller than d and the wavelength λ of the generated electromagnetic wave.

These two models can be considered as among the most fundamental that can radiate a directed electromagnetic wave. Hence, they are the most fundamental models enabling generation of electromagnetic propulsion. When several dipoles have arbitrary locations and orientations, propulsion can be obtained from the analysis of these models. In the following, based on the terminology of antenna engineering [11], these models are called the CA (colinear-type array) model [Fig. 1(a)] and the PA (parallel-type array) model [Fig. 1(b)].

2.2. Electromagnetic field formed by two dipoles

The components of the electromagnetic fields formed at a certain point P by a dipole P_1 located at the origin are given by the following equations common to both models:

$$E_{1x} = \frac{P_1(t)}{4\pi\varepsilon_0} e^{-jkr} \left(\frac{3}{r^3} + \frac{3jk}{r^2} - \frac{k^2}{r} \right) \sin\theta \cos\theta \cos\varphi$$
$$E_{1y} = \frac{P_1(t)}{4\pi\varepsilon_0} e^{-jkr} \left(\frac{3}{r^3} + \frac{3jk}{r^2} - \frac{k^2}{r} \right) \sin\theta \cos\theta \sin\varphi$$
$$E_{1z} = \frac{P_1(t)}{4\pi\varepsilon_0} e^{-jkr} \left\{ \left(\frac{3}{r^3} + \frac{3jk}{r^2} - \frac{k^2}{r} \right) \cos^2\theta - \left(\frac{1}{r^3} + \frac{jk}{r^2} - \frac{k^2}{r} \right) \right\}$$
$$H_{1x} = \frac{\omega P_1(t)}{4\pi} e^{-jkr} \left(-\frac{j}{r^2} + \frac{k}{r} \right) \sin\theta \sin\varphi$$
$$H_{1y} = \frac{\omega P_1(t)}{4\pi} e^{-jkr} \left(\frac{j}{r^2} - \frac{k}{r} \right) \sin\theta \cos\varphi$$
$$H_{1z} = 0 \quad (2)$$

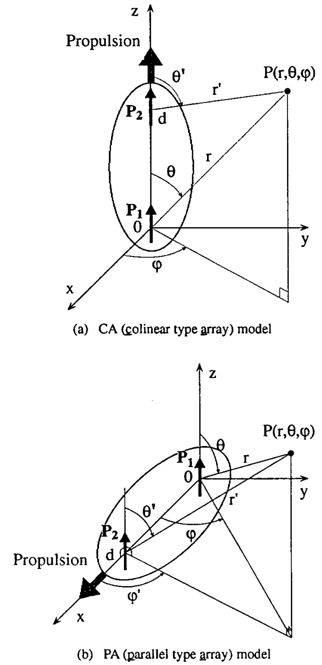

Fig. 1. Two basic models for analysis.

where ε_0 is the permittivity of a vacuum, k is the wave number of the generated electromagnetic wave, and $k = \omega / c$ (c: speed of light in vacuum).

These electromagnetic fields can be divided into three components. They are the static electric field related to $1/r^3$, the inductive electromagnetic field related to $1/r^2$, and the radiated electromagnetic field related to $1/r$. Of these components, the radiated electromagnetic field is the propagating component and is dominant in the region sufficiently away from the source. The remaining two components are nonpropagating components effective near the source.

The electromagnetic field components E_{2i} and H_{2i}($i = x, y, z$) generated at point P by dipole P_2 can be obtained by replacing $P_1(t)$, r, θ, φ, with $P_2(t)$, r', θ', φ'.

The electromagnetic fields E_i and H_i generated at point P by the two dipoles P_1 and P_2 can be expressed as the sums of individual components:

$$E_i = E_{1i} + E_{2i}, \quad H_i = H_{1i} + H_{2i} \quad (i = x, y, z) \tag{3}$$

From the geometric relationship in Fig. 1, the following relationships exist in each model between r, θ, φ and r', θ', φ':

[CA model]

$$\begin{aligned} r'\sin\theta' &= r\sin\theta \\ r'\cos\theta' &= r\cos\theta - d \\ \varphi' &= \varphi \end{aligned} \tag{4}$$

[PA model]

$$\begin{aligned} r'\sin\theta'\cos\varphi' &= r\sin\theta\cos\varphi - d \\ r'\sin\theta'\sin\varphi' &= r\sin\theta\sin\varphi \\ r'\cos\theta' &= r\cos\theta \end{aligned} \tag{5}$$

3. Analysis

3.1. Fundamental equations for electromagnetic propulsion

The force $\boldsymbol{F}$ exerted on a system placed in an electromagnetic field can be expressed as follows in terms of Maxwell's stress tensor $\boldsymbol{T}$ and the electromagnetic momentum density $\boldsymbol{g}$:

$$\boldsymbol{F} = \iint_S (\boldsymbol{T}\cdot\boldsymbol{n})\, ds - \frac{d}{dt}\iiint_V \boldsymbol{g}\, dv \tag{6}$$

where S is the surface area of V, and $\boldsymbol{n}$ is the normal vector of S. Here, the component T_{ij} of $\boldsymbol{T}$ and $\boldsymbol{g}$ can be expressed as follows in terms of the electric field $\boldsymbol{E}$, the magnetic field $\boldsymbol{H}$, the electric flux density $\boldsymbol{D}$, and the magnetic flux density $\boldsymbol{B}$:

$$T_{ij} = E_i D_j + H_i B_j - \frac{1}{2}(\boldsymbol{E}\cdot\boldsymbol{D} + \boldsymbol{H}\cdot\boldsymbol{B})\,\delta_{ij} \quad (i, j = x, y, z)$$

$$\boldsymbol{g} = \boldsymbol{D}\times\boldsymbol{B} = \frac{1}{c^2}\boldsymbol{E}\times\boldsymbol{H} \tag{7}$$

The first term on the right-hand side of Eq. (6) represents the electromagnetic momentum flowing into V through S per unit time, while the second term represents the increment of the electromagnetic momentum in V per unit time. Hence, the force $\boldsymbol{F}$ may be interpreted as the electromagnetic momentum that has vanished in V per unit time.

From the spatial symmetry of the electromagnetic field in each analysis model, it is considered that a propulsion is generated along the z axis in the CA model and along the x axis in the PA model. Further, let us consider the time average $\overline{F}_i$ [$i = z$ (CA model), x (PA model)] of the component of $\boldsymbol{F}$ in Eq. (6) along the direction of propulsion in order to derive only the effective propulsion component.

In the steady state of each analysis model, the time average of the electromagnetic momentum in V is constant. Hence, the second term on the right-hand side of Eq. (6) is 0. Therefore, the propulsion to be derived is as follows:

$$\begin{aligned} \overline{F}_i &= \iint_S (\overline{\boldsymbol{T}}\cdot\boldsymbol{n})_i\, ds \\ &= \iint_S \left(\overline{T_{ix}}\, n_x + \overline{T_{iy}}\, n_y + \overline{T_{iz}}\, n_z\right) ds \\ &[i = z\ (\text{CA model}),\ x\ (\text{PA model})] \end{aligned} \tag{8}$$

where the bar above the symbol indicates the time average.

3.2. Analysis of CA model

Let the spherical surface with a radius r centered at the origin (dipole P_1) be the integration range S. It is assumed that r is sufficiently larger than the dipole spacing d and the wavelength λ of the generated electromagnetic field.

The normal vector to this spherical surface is given by

$$\boldsymbol{n} = (n_x, n_y, n_z) = (\sin\theta\cos\varphi, \sin\theta\sin\varphi, \cos\theta) \tag{9}$$

Hence, if the first expressions in Eqs. (7) and (9) are applied to Eq. (8),

$$\begin{aligned} \overline{F}_z &= \iint_S \left(\overline{T_{zx}}\, n_x + \overline{T_{zy}}\, n_y + \overline{T_{zz}}\, n_z\right) ds \\ &= \int_0^{2\pi} d\varphi \int_0^{\pi} d\theta\cdot r^2\sin\theta \\ &\times\Big[\varepsilon_0\, \overline{E_x E_z}\sin\theta\cos\varphi + \varepsilon_0\, \overline{E_y E_z}\sin\theta\sin\varphi \\ &+ \left\{\frac{\varepsilon_0}{2}\left(\overline{E_z^2} - \overline{E_x^2} - \overline{E_y^2}\right) - \frac{\mu_0}{2}\left(\overline{H_x^2} + \overline{H_y^2}\right)\right\}\cos\theta\Big] \end{aligned} \tag{10}$$

where μ_0 is the permeability of vacuum.

From the condition of integration range $r >> d$ and from Eq. (4), the following relationship is derived:

$$r' \approx r\left(1 - \frac{d}{r}\cos\theta\right) \approx r, \quad r - r' \approx d\cos\theta, \quad \theta' \approx \theta \tag{11}$$

The above and the condition for the integration range $kr >> 1 (r >> \lambda)$ are applied to Eqs. (2) and (3), and then the results are substituted into Eq. (10). Further, by means of time averaging, the terms with perturbation in time are eliminated:

$$\begin{aligned} \overline{F}_z &= -\frac{p_1 p_2}{16\pi^2\varepsilon_0} k^4 \int_0^{2\pi} d\varphi \int_0^{\pi} d\theta \\ &\times\left[\left\{1 + \cos(kd\cos\theta + \alpha)\right\}\sin^3\theta\cos\theta\right] \end{aligned} \tag{12}$$

From the above, the electromagnetic propulsion in the CA model can be derived as follows:

$$\overline{F}_z = \frac{p_1 p_2}{4\pi\varepsilon_0}\left\{\left(\frac{6}{d^4} - \frac{2k^2}{d^2}\right)\sin(kd) - \frac{6k}{d^3}\cos(kd)\right\}\sin\alpha \tag{13}$$

3.3. Analysis of PA model

Let us consider the integration the same as that for the CA model. From Eq. (8) and the first expression in Eq. (7) together with Eq. (9), the following is obtained:

$$\begin{aligned} \overline{F}_x &= \iint_S \left(\overline{T_{xx}}\, n_x + \overline{T_{xy}}\, n_y + \overline{T_{xz}}\, n_z\right) ds \\ &= \int_0^{2\pi} d\varphi \int_0^{\pi} d\theta\cdot r^2\sin\theta \\ &\times\Big[\left\{\frac{\varepsilon_0}{2}\left(\overline{E_x^2} - \overline{E_y^2} - \overline{E_z^2}\right) + \frac{\mu_0}{2}\left(\overline{H_x^2} - \overline{H_y^2}\right)\right\}\sin\theta\cos\varphi \\ &+ \left(\varepsilon_0\, \overline{E_x E_y} + \mu_0\, \overline{H_x H_y}\right)\sin\theta\sin\varphi + \varepsilon_0\, \overline{E_x E_z}\cos\theta\Big] \end{aligned} \tag{14}$$

When the condition $r >> d$ for the integration range is applied to Eq. (5), the following relationships hold:

$$\begin{aligned} &r' \approx r\left(1 - \frac{d}{r}\sin\theta\cos\varphi\right) \approx r, \quad r - r' \approx d\sin\theta\cos\varphi \\ &\theta' \approx \theta, \quad \varphi' \approx \varphi \end{aligned} \tag{15}$$

The above and the condition $kr >> 1 (r >> \lambda)$ are applied to Eqs. (2) and (3). The results are substituted into Eq. (14) and the time averaging is taken. Then,

$$\begin{aligned} \overline{F}_x &= -\frac{p_1 p_2}{16\pi^2\varepsilon_0} k^4 \int_0^{2\pi} d\varphi \int_0^{\pi} d\theta \\ &\times\left[\left\{1 + \cos(kd\sin\theta\cos\varphi + \alpha)\right\}\sin^4\theta\cos\varphi\right] \end{aligned} \tag{16}$$

From the above, the electromagnetic propulsion of the PA model is derived as follows:

$$\overline{F}_x = \frac{p_1 p_2}{4\pi\varepsilon_0}\left\{\left(-\frac{3}{d^4} + \frac{2k^2}{d^2}\right)\sin(kd) + \left(\frac{3k}{d^3} - \frac{k^3}{d}\right)\cos(kd)\right\}\sin\alpha \tag{17}$$

4. Discussion

4.1. Dependence of electromagnetic propulsion on the spacing between dipoles

From expressions (13) and (17) for the propulsion, it is found that the magnitude of the propulsion is proportional to $\sin\alpha$ and reaches a maximum when the phase difference α of the two dipoles is $\pi/2$ or $3\pi/2$. When $\sin\alpha \neq 0$ and the wave number k is constant, the variation of the propulsion versus the dipole spacing d is as shown in Fig. 2. As d becomes larger, the propulsion decreases toward 0 with positive and negative undulations. The undulation is due to the portions related to the phase difference in Eqs. (13) and (17), $\sin(kd)$ and $\cos(kd)$. Also, the amplitude becomes smaller in inverse proportion to the power of d. As d becomes larger, the propulsion approaches 0. This is attrib-

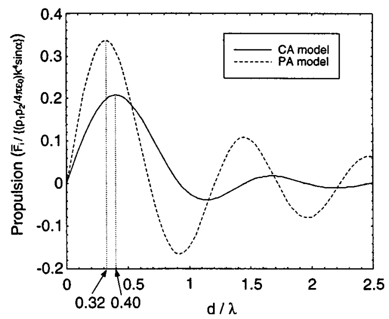

Fig. 2. Dependence of propulsion on d.

uted to the reduction of the directed radiation component as the interaction between the two dipoles becomes smaller.

As shown in Fig. 2, the propulsion becomes the largest for certain characteristic values of the distance $d_{F\max}$ between the dipoles in each model. $d_{F\max}$ can be derived analytically from Eqs. (13) and (17) and are given as follows:

[CA model]

From

$$\tan(kd_{F\max}) + \frac{-(kd_{F\max})^3 + 12kd_{F\max}}{5(kd_{F\max})^2 - 12} = 0 \qquad (18)$$

one finds

$$d_{F\max} \approx 0.40\lambda \qquad (19)$$

[PA model]

From

$$(kd_{F\max})^2 - 4 = 0 \qquad (20)$$

one obtains

$$d_{F\max} = \frac{1}{\pi}\lambda \approx 0.32\lambda \qquad (21)$$

On the other hand, there exists a distance d_{F0} where the propulsion becomes 0. This can be found from the following that can be obtained from Eqs. (13) and (17).

[CA model]

$$\tan(kd_{F0}) + \frac{3kd_{F0}}{(kd_{F0})^2 - 3} = 0 \qquad (22)$$

[PA model]

$$\tan(kd_{F0}) + \frac{3kd_{F0} - (kd_{F0})^3}{2(kd_{F0})^2 - 3} = 0 \qquad (23)$$

Especially at the limit of $d \to 0$, Eqs. (13) and (17) become 0. This is because the two dipoles behave as though they are one dipole with an amplitude dependent on the phase difference α as d approaches 0 so that the directed radiating component is lost.

4.2. Relationship between electromagnetic propulsion and radiated power

The electromagnetic propulsion recognized as the counteraction by radiation is expected to have a relationship with the radiated power W of the electromagnetic wave radiated from the source. Poynting vectors obtained from Eqs. (2) and (3) are surface-integrated over a spherical surface in the far zone as in the derivation of the propulsion. If the total radiated power W is derived,

$$W = \iint_S \left(\overline{\boldsymbol{E}\times\boldsymbol{H}}\right)\cdot \boldsymbol{n}\, dS \qquad (24)$$

the following is obtained for each model.

[CA model]

$$W_{CA} = \frac{ck^4}{4\pi\varepsilon_0}\left[\frac{p_1^2}{3} + \frac{p_2^2}{3} + p_1p_2\left\{\frac{2}{(kd)^3}\sin(kd) - \frac{2}{(kd)^2}\cos(kd)\right\}\cos\alpha\right] \qquad (25)$$

[PA model]

$$W_{PA} = \frac{ck^4}{4\pi\varepsilon_0}\left[\frac{p_1^2}{3} + \frac{p_2^2}{3} + p_1p_2\left\{\left(-\frac{1}{(kd)^3} + \frac{1}{kd}\right)\sin(kd) + \frac{1}{(kd)^2}\cos(kd)\right\}\cos\alpha\right] \qquad (26)$$

In Fig. 3, the d dependence of the radiated power with several values of phase difference α is shown for $p_1 = p_2 = p$. The vertical axis is normalized to the radiated power $(p^2/4\pi\varepsilon_0)ck^4/3$ of one dipole with an amplitude of p.

Let us differentiate the radiated powers W_{CA} and W_{PA} with respect to d so that the increments W'_{CA} and W'_{PA} with respect to d are obtained.

[CA model]

$$W'_{CA} = -\frac{p_1p_2}{4\pi\varepsilon_0}ck\left\{\left(\frac{6}{d^4} - \frac{2k^2}{d^2}\right)\sin(kd) - \frac{6k}{d^3}\cos(kd)\right\}\cos\alpha \qquad (27)$$

[PA model]

$$W'_{PA} = -\frac{p_1p_2}{4\pi\varepsilon_0}ck\left\{\left(-\frac{3}{d^4} + \frac{2k^2}{d^2}\right)\sin(kd) + \left(\frac{3k}{d^3} - \frac{k^3}{d}\right)\cos(kd)\right\}\cos\alpha \qquad (28)$$

In Eqs. (27) and (28), the expression inside the braces has the same form as that inside the braces in Eqs. (13) and (17) for the propulsion. In the case of $\cos\alpha \neq 0$, the propulsion becomes 0 when the increment of the radiated power with respect to d is 0. When the magnitude of the increment of the radiated power is maximum (or the inflection point in Fig. 3), the magnitude of the propulsion becomes the maximum or a maximum.

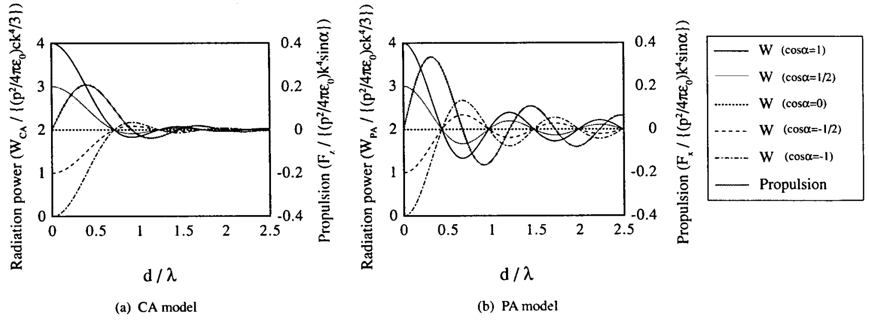

Fig. 3. Relation between radiation power and propulsion ($p_1 = p_2 = p$).

In the case of $\cos\alpha = 0$, the radiated power is constant regardless of d. Then, the magnitude of the propulsion exhibits the largest value ($\sin\alpha = \pm 1$) as a function of α. While the total radiated power is kept constant, only the radiation pattern changes so that the d dependence of the propulsion occurs. Figure 4 shows an example of the radiation pattern (electric field intensity) in the far field region. When $d = d_{F\max}$, the propulsion becomes the largest. Then, from Eqs. (13), (17), (25), and (26), the propulsion per radiated power becomes the largest for $p_1 = p_2$. For $\cos\alpha = 0$, $d = d_{F\max}$, and $p_1 = p_2$, the magnitude of the propulsion for 1 W of radiated power becomes 1.04 nN in the CA model and 1.68 nN in the PA model.

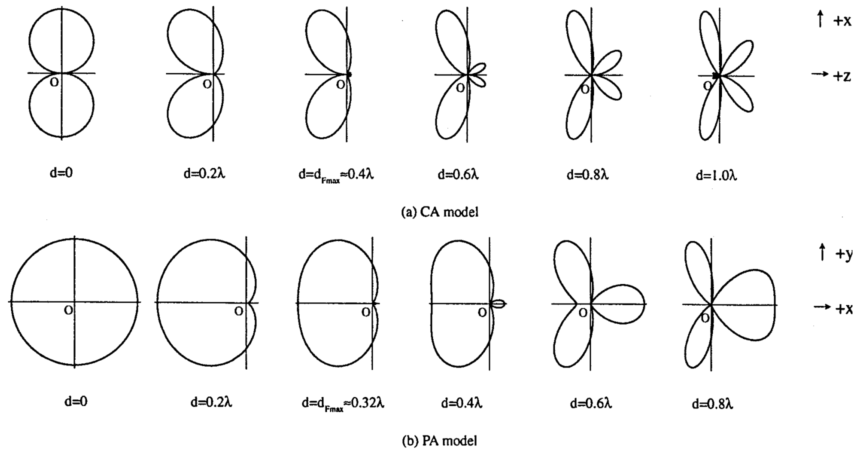

Fig. 4. Radiation pattern (field pattern) ($p_1 = p_2$, $\alpha = \pi/2$).

4.3. Interpretation of electromagnetic propulsion

The expressions (13) and (17) for the propulsion have a form in which the term $k^{(4-n)}/d^n (n = 1 \sim 4)$ is multiplied by $\sin(kd)$, $\cos(kd)$, and $\sin\alpha$, related to the phase difference. In particular, the term of $1/d^4$ has the form of a product with $\sin(kd)\sin\alpha$, related to the phase of the Coulomb force $(p_1p_2/4\pi\varepsilon_0)(6/d^4)$ (CA model) or $-(p_1p_2/4\pi\varepsilon_0)(3/d^4)$ (PA model).

These forms can be explained by the dipole as the acting point of the force and the propagation delay of the electromagnetic wave formed by the facing dipole. Let us consider the CA model by using Fig. 5. In the CA model, the dipole as the acting point of the force is located on the z axis. Also, from Eq. (2), only the z component of the electric field exists on the z axis. Further, of the z component of the electric field, only the near field, that is, the static electric field and inductive electromagnetic field, exists. The electric field formed by the dipole P_2 at a certain point on the z axis is expressed by $E_2(r', t)$ as a function of distance r' from P_2 and time t. Then, the electric field $E_2(r', t)$ is proportional to $P_2(t - r'/c)$ as shown below. This r'/c is the propagation delay time of the electromagnetic wave from P_2 to the point at distance r':

$$E_2(r', t) = \frac{P_2(t)}{4\pi\varepsilon_0} e^{-jkr'}\left\{\frac{2}{r'^3} + \frac{2jk}{r'^2}\right\} = \frac{P_2\left(t - \frac{r'}{c}\right)}{4\pi\varepsilon_0}\left\{\frac{2}{r'^3} + \frac{2jk}{r'^2}\right\} \tag{29}$$

Here, let us assume that the internal structure of the dipole $P_n (n = 1, 2)$ consists of a positive and a negative charge separated by an infinitesimal distance $l (l << d, kl << 1)$. Then, $P_n(t)$ is given as follows:

$$P_n(t) = Q_n(t)\, l \quad (n = 1, 2) \tag{30}$$

From Eqs. (29) and (30), the force $F_1(t)$ that the dipole P_1 receives from the electric field $E_2(r', t)$ at time t can be derived as follows:

$$F_1(t) = Q_1(t)\, E_2\left(d - \frac{l}{2}, t\right) - Q_1(t)\, E_2\left(d + \frac{l}{2}, t\right) \approx \frac{P_1(t) P_2\left(t - \frac{d}{c}\right)}{4\pi\varepsilon_0}\left\{\frac{6}{d^4} + \frac{6jk}{d^3} - \frac{2k^2}{d^2}\right\} \tag{31}$$

$F_1(t)$ is proportional to $P_1(t)P_2(t - d/c)$. [See Fig. 5(a).]

Similarly, the magnitude of the force $F_2(t)$ that the dipole P_2 receives is proportional to $P_1(t - d/c)P_2(t)$ [as seen in Fig. 5(b)] and is given by the following:

$$F_2(t) = Q_2(t)\, E_1\left(d + \frac{l}{2}, t\right) - Q_2(t)\, E_1\left(d - \frac{l}{2}, t\right) \approx \frac{P_1\left(t - \frac{d}{c}\right) P_2(t)}{4\pi\varepsilon_0}\left\{-\frac{6}{d^4} + \frac{6jk}{d^3} - \frac{2k^2}{d^2}\right\} \tag{32}$$

The force $F_{total}(t)$ working on the system consisting of two dipoles is obtained as the sum of $F_1(t)$ and $F_2(t)$. [See Fig. 5 (c).] This is obtained as follows:

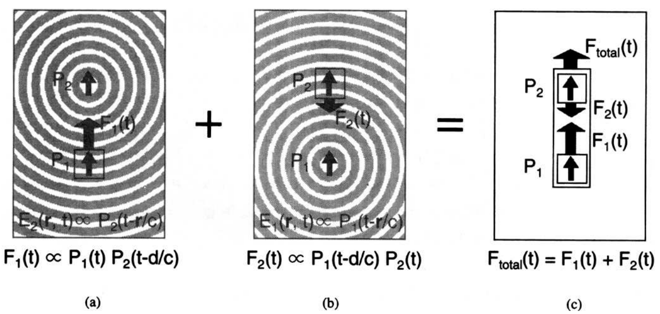

Fig. 5. An explanation of electromagnetic propulsion (CA model). (a) Force $F_1(t)$ acting on P_1 in electric field E_2. The concentric circle shows electric field E_2 caused by P_2. (b) Force $F_2(t)$ acting on P_2 in electric field E_1. (c) Force $F_{\text{total}}(t)$ acting on the two-dipole system which is given by total of $F_1(t)$ and $F_2(t)$. See text for further details.

$$F_{total}(t) = F_1(t) + F_2(t) = \frac{P_1P_2}{4\pi\varepsilon_0}\left\{\left(\frac{6}{d^4} - \frac{2k^2}{d^2}\right)\sin(kd) - \frac{6k}{d^3}\cos(kd)\right\}\sin\alpha \tag{33}$$

This result is identical to Eq. (13). At each dipole as an acting point of the force, the magnitude of the forces at the same instant is the difference due to propagation delay of the electromagnetic waves generated by the opposing dipoles, and the difference constitutes propulsion.

From the calculation process of Eqs. (31), (32), and (33), it is found that the first term ($1/d^4$) on the right-hand side of Eq. (13) is caused by the static field, the second term (k^2/d^2) by the inductive electromagnetic field, and the third term (k/d^3) by the static electric field and the inductive electromagnetic field. In the CA model, only the near field becomes a source of propulsion.

Details are described above for the CA model. For the PA model, Eq. (17) can be derived from a similar analysis. The first term on the right-hand side of Eq. (17) is caused by the static electric field, the second term by the inductive electromagnetic field and the radiated electromagnetic field, the third term by the inductive electromagnetic field, and the fourth term by the radiated electromagnetic field.

In each model, the near field contributes to the propulsion. The electromagnetic momentum corresponding to the propulsion is finally carried away by the radiated electromagnetic field and is recognized as directed electromagnetic radiation.

5. Conclusions

In regard to two types of systems made of two dipoles (CA model and PA model), the electromagnetic propulsion generated in these systems was analyzed and studied.

The origin of the propulsion is related to the near fields, such as the static electric field and the inductive electromagnetic field. The electromagnetic momentum flow corresponding to the propulsion travels a far distance through the radiated electromagnetic field.

Even for directed electromagnetic radiation, the near field is related to the origin. This finding can provide a clue to the construction of a physical image for conversion of evanescent light to propagating light between a probe and a sample, as reported for the near-field optical microscope [9, 10, 12].

In the future, it is planned to attempt a representation of the electromagnetic propulsion in a more general model. By using these analytical results, specific applications to near-field optics and micromachines are possible.

REFERENCES

1. Ashkin A. Acceleration and trapping of particles by radiation pressure. Phys Rev Lett 1970;24:156–159.
2. Gordon JP. Radiation forces and momenta in dielectric media. Phys Rev A 1973;8:14–21.
3. Ashkin A. Application of laser radiation pressure. Science 1980;210:1081–1088.
4. Marx G. Interstellar vehicle propelled by terrestrial laser beam. Nature 1966;211:22–23.
5. Moeckel WE. Propulsion by impinging laser beams. J Space Rockets 1972;9:942–944.
6. Forward RL. Roundtrip interstellar travel using laser-pushed lightsails. J Spacecr Rockets 1984;21:187–195.
7. Forward RL. Starwisp: An ultra-light interstellar probe. J Spacecr Rockets 1985;22:345–350.
8. Stenholm S. The semiclassical theory of laser cooling. Rev Mod Phys 1986;58:699–739.
9. Ohtsu M. Progress of high-resolution photon scanning tunneling microscopy due to a nanometric fiber probe. IEEE J Lightwave Technol 1995;13:1–22.
10. Hori Y. Photon scanning tunneling microscope and its theoretical interpretation. Appl Phys 1992;61:612–616.
11. I.E.I.C.E. Antenna Engineering Handbook. Ohm Press, p. 198, 1994
12. IEICE. Antenna engineering handbook. Solid State Phys 1998;33:395–403.

AUTHORS (from left to right)

Noriaki Obara (member) graduated from the Department of Applied Physics, Tohoku University, in 1990 and joined the Communications Research Laboratory, Ministry of Posts and Telecommunications. Since then, he has been engaged in research on antennas for satellite communication and on propagation. He also has an interest in the fundamental theory of electromagnetic fields. From 1993 to 1995, he was a member of the 35th Japanese Antarctic Research Expedition and was engaged in observation of upper atmosphere physics. In 1999, he completed a doctoral course at Iwate University. He holds a D.Eng. degree. Presently, he is with Satellite Communications Section, Kashima Space Research Center. He is a member of the Japan Society of Applied Physics.

Mamoru Baba completed a doctoral course (majoring in electronic engineering) at Tohoku University in 1974 and became a researcher at Toshiba R&D Center. In 1976, he became a research associate in the Department of Electronic Engineering, Iwate University and is presently a professor in the Department of Electrical and Electronic Engineering. He holds a D.Eng. degree. He has been engaged in research on photonic properties of inorganic materials, semiconductor photoelectronic devices, and metal oxide thin film devices. He is a member of the Japan Society of Applied Physics and the Japan Physical Society.